1992

Performance of test embankment constructed to failure on soft marine clay

Buddhima Indraratna
University of Wollongong, indra@uow.edu.au

A S. Balasubramaniam

S Balachandran
Inst Tech Sri Lankan

Publication Details

Indraratna, B, Balasubramaniam, AS and Balachandran, S, Performance of test embankment constructed to failure on soft marine clay, International Journal of Geotechnical Engineering, 118(1), 1992, 12-33.

Performance of Test Embankment Constructed to Failure on Soft Marine Clay

By B. Indraratna,[1] Member, ASCE, A. S. Balasubramaniam,[2] Fellow, ASCE, and S. Balachandran[3]

Abstract: This paper describes the observed and the predicted performance of a full-scale trial embankment built to failure on a soft Malaysian marine clay. Predictions of the subsoil deformation, the critical height of fill and the corresponding slip surface are made and subsequently compared to the field measurements. It is of importance to realize that all the predictions were made prior to the actual failure of the embankment. The comparison with measurements was possible only after the International Symposium on Trial Embankments on Malaysian Marine Clays, was held in Kuala Lumpur, Malaysia, in November 1989, during which the field data were made available to the invited predictors (including the second writer) by the Malaysian Highway Authority. Finite-element codes based on the modified Cam-clay theory (CRISP) and hyperbolic stress-strain model (ISBILD) were utilized to investigate the behavior of the embankment and the foundation soil until failure. The type of numerical modeling includes purely undrained, fully drained, and a coupled consolidation analysis. The finite-element solutions are subsequently compared with the conventional stability analysis.

Introduction

The rapid-development strategies and the associated urbanization in certain parts of Malaysia have compelled engineers to construct earth structures such as embankments and major highways over soft clay deposits having low bearing capacities coupled with excessive settlement characteristics. In Southeast Asia soft clays are fairly widespread, and some of these deposits exist extensively in the vicinity of capital cities. The construction of the Malaysian North-South Expressway across the Muar plain has met formidable obstacles (instability) where a significant part of the expressway crosses over 10–20 m of thick soft clay deposits characterized by low undrained shear strengths and high water contents. Furthermore, ground subsidence associated with the consolidation of soft clay deposits also pose considerable threats to surface structures.

To investigate in detail the behavior of Muar clay deposits, the Malaysian Highway Authority recently selected an appropriate site on the Muar plain to construct several full-scale test embankments, with one built to failure. The clays along the west coast of Peninsular Malaysia constitute a coastal plain marine clay up to 20 m thick, with an average lateral extent of about 25 km. The site of the test embankment is located about 20 km inland from Muar and 50 km due east of Malacca on the southwest coast of Malaysia (Fig. 1). The subsurface geology data at the site reveal the existence of a

[1]Lec., Dept. of Civ. and Mining Engrg., Univ. of Wollongong, P.O. Box 1144 (Northfields Ave.), Wollongong, NSW 2500, Australia.

[2]Prof., Div. of Geotech. Engrg., Asian Inst. of Tech., G.P.O. Box 2754, Bangkok, Thailand.

[3]Grad. Student, Univ. of Cambridge, Cambridge, CB2 1ST England.

Note. Discussion open until June 1, 1992. To extend the closing date one month, a written request must be filed with the ASCE Manager of Journals. The manuscript for this paper was submitted for review and possible publication on January 7, 1991. This paper is part of the *Journal of Geotechnical Engineering*, Vol. 118, No. 1, January, 1992. ©ASCE, ISSN 0733-9410/92/0001-0012/$1.00 + $.15 per page. Paper No. 1215.

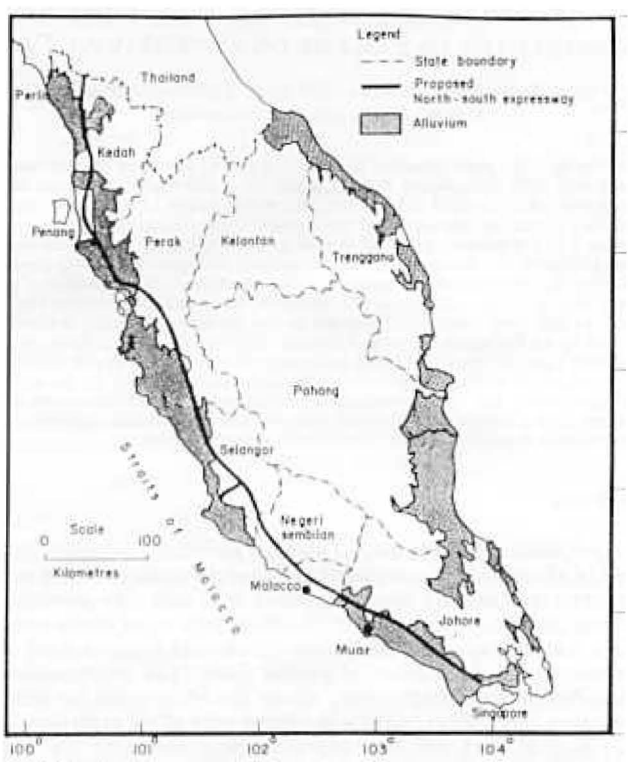

FIG. 1. River and Coastal Alluvium of Peninsular Malaysia

weathered crust of about 2.0 m thick above a 16.5 m thick layer of soft silty clay. The latter layer can be further divided into an upper very soft and a lower soft silty clay. Immediately beneath this lower clay layer is a 0.3–0.5 m thick peaty soil followed by a stiff sandy clay. The clayey succession ends at a dense sand layer at about 22.5 m below ground level. Although many soft clays encountered in the Southeast Asian countries are generally normally consolidated, they may exhibit light overconsolidation caused by surface desiccation and weathering. The apparent overconsolidation ratio (OCR) of such a clay can be as high as 2.5, and this influences its preconsolidation pressure and undrained strength (Bjerrum 1973).

The embankment raised on this soft Muar clay formation failed by the development of a "quasi slip circle" type of rotational failure at a critical height of approximately 5.5 m, with a pronounced tension crack propagating vertically through the crust and the fill (Figs. 2 and 3). This paper elucidates the predicted behavior of the soft Muar clay foundation with regard to the critical height of embankment at failure, excess pore pressures, lateral and vertical displacements (including heave), as well as an attempt to propose a conceivable failure mode. The predictions are made on the basis of several deformation analyses incorporating two different constitutive soil models,

FIG. 2. View of Tensile Fracture of Compacted Fill

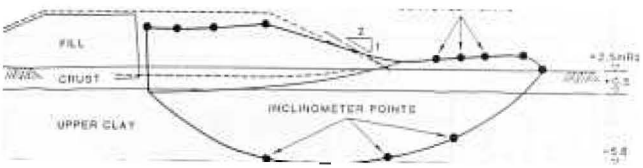

FIG. 3. Failure Mode of Embankment and Foundation (Brand and Premchitt 1989)

based on the modified Cam-clay theory and the hyperbolic stress-strain behavior. From the numerical [finite-element method (FEM)] analysis, predictions of displacements and pore pressures were made and subsequently compared with the field measurements obtained at various locations within the subsoil and the embankment. The zones of yielding and the potential failure surface are interpreted based on the locations of critical shear-stress ratios and maximum displacement vectors. The actual failure surface was identified by the Malaysian Highway Authority, by a combined topographical survey and inclinometer response within the upper clay layer, as illustrated in Fig. 3.

MUAR TEST EMBANKMENT

Soil conditions

The ground profile, the soil description and some properties at the site of the test embankment are given in Table 1. Fig. 4 summarizes the available detailed test data such as the water contents, Atterberg limits, vane shear strengths, and the cone-penetration resistance of the soft Muar clay to a depth of about 17.5 m below ground level. A relatively stiff but brittle thin crust (less than 2.5 m) exists on top of the very soft Muar clay layer, below

TABLE 1. Soil Profile and Soil Properties at the Muar Test Embankment Site (Data Provided by Malaysian Highway Authority)

Depth (m) (1)	Soil Description (2)	Soil Description (3)	Dominant minerals determined by X-ray diffraction (4)	Grain Size (%) Clay (5)	Silt (6)	Sand (7)	Gravel (8)	Coefficient of horizontal permeability, k_h (m/sec) (9)	Compression ratio ($C_c/1 + e_o$) (10)	Preconsolidation pressure, P_c (kPa) (11)
—	—	—	—	—	—	—	—	—	—	—
	Crust	Yellowish brown mottled red clay with roots, root holes, and laterite concretions	—	62	35	3	0	—	0.3	110
	Upper clay	Light greenish gray clay with a few shells, very thin discontinuous sand partings, occasional near vertical roots and some decaying organic matter (less than 2%)	Kaolinite, montmorillonite, illite, quartz	45	52	3	0	4×10^{-9}	0.5	40
	Lower clay	Gray clay with some shells, very thin discontinuous sand partings and some decaying organic matter (less than 2%)	Kaolinite, montmorillonite, illite, quartz	50	47	3	0	10^{-9}	0.3	60
	Peat	Dark brown peat with no smell (carbon dated to 10,000 years BP)	—	—	—	—	—	—	—	
−15.9 m	Sandy clay	Grayish brown sandy clay with a little decaying organic matter	—	20	36	44	0	2×10^{-7}	0.1	60
−19.9 m	Sand	Dark gray very silty medium to coarse sand (standard penetration test greater than 20)	—	4	20	71	5	—	—	

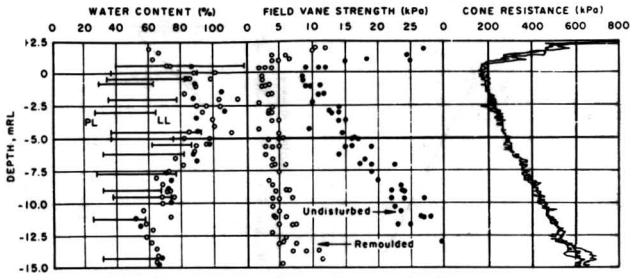

FIG. 4. Variation of Soil Properties with Depth

which the water content is as high as 100% and generally exceeds the liquid limit. The plasticity index generally ranges between 40% and 50%. The undrained shear strength as measured by the field vane has a minimum value of about 8 kPa at a depth of 3 m, and this increases approximately linearly with depth. The cone resistance not only indicates a similar trend, but also reflects clearly the influence of the crust (Brand and Premchitt 1989). Very little information is available with regard to the thin peaty soil layer (less than 0.5 m thick) at a depth of about 18 m below the ground level.

In addition to the extensive in-situ data, a considerable amount of laboratory information was acquired for the subsurface clay deposits prior to the construction of the test embankment. Apart from the determination of detailed physical characteristics, extensive laboratory tests were conducted at the Asian Institute of Technology, in Bankok, to measure their engineering properties. These include direct shear tests, unconfined compression tests, unconsolidated undrained (UU) triaxial tests, and consolidated undrained (CIU) and consolidated drained (CD) triaxial tests. Laboratory permeability tests and oedometer consolidation tests were also carried out. A summary of the undrained shear-strength profiles and permeability measurements are illustrated in Figs. 5 and 6, respectively. Except for the direct shear test, the laboratory results closely resemble the field vane shear-strength profile.

The field measurements were used in the numerical analysis after being subjected to correction factors suggested by Bjerrum (1973). The undrained modulus (E_u) and effective strength parameters (c', ϕ'), were also determined from the appropriate triaxial tests, and are summarized in Table 2 for the various clay layers. In addition to these routine geotechnical tests, a series of specialized triaxial tests were conducted, including constant stress ratio tests, effective and total stress path tests, and anisotropically consolidated undrained (CU) tests. These tests were intended to provide the most appropriate modified Cam-clay model parameters (Table 3) for the prediction of displacements and pore-pressure changes associated with the various clay layers beneath the test embankment.

Finite Element Codes and Soil Models

Modified Cam-Clay Model in CRISP

CRISP, a critical-state finite-element program developed at Cambridge University, Cambridge, England, has been used extensively to analyze geo-

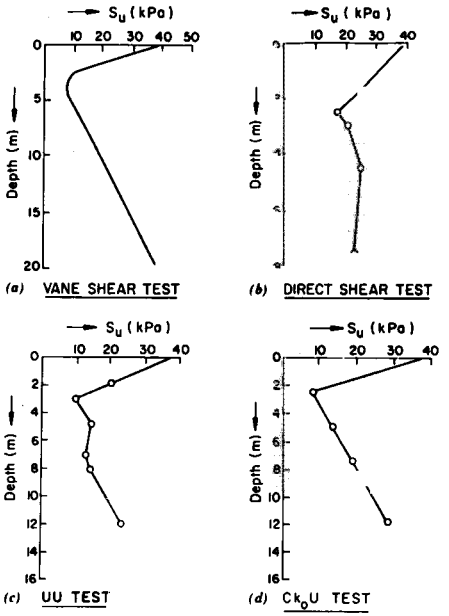

FIG. 5. Shear-Strength Profiles from Different Types of Tests

technical problems. This program allows undrained, drained, or fully coupled (Biot) consolidation analyses. The coupled consolidation model incorporates the undrained modified Cam-clay deformations and the drained consolidation settlements. The modified Cam-clay model generalized by Roscoe and Burland (1968), was selected as the constitutive model appropriate for Muar clay formations. Both undrained and coupled consolidation analyses (plane strain) were carried out by the finite-element method utilizing linear-strain triangular elements characterized by additional pore-pressure degrees of freedom in order to compute lateral and vertical displacements, excess pore-water pressures, surface settlements, and shear-stress distributions corresponding to the sequential construction of the test embankment.

FEM (CRISP) descretization of the test embankment and its foundation for both undrained and coupled consolidation models is shown in Fig. 7. A foundation depth of 22.5 m was considered adequate for the purpose of analysis because of the existence of a dense sand layer beneath the clayey deposits. The lateral boundary of the finite-element mesh is defined by a distance of three times the vertical depth from the toe of the embankment. The clay foundation is divided into eight horizontal layers of elements, simulating the characteristic properties of the different soil deposits.

The necessary critical state parameters, λ, κ, M, and N (Roscoe and Burland 1968) are graphically represented in Fig. 8. For the finite-element code based on the modified Cam-clay model, the associated soil deformation can be defined by determining these parameters correctly. The procedure for the determination of these four fundamental Cam-clay parameters by

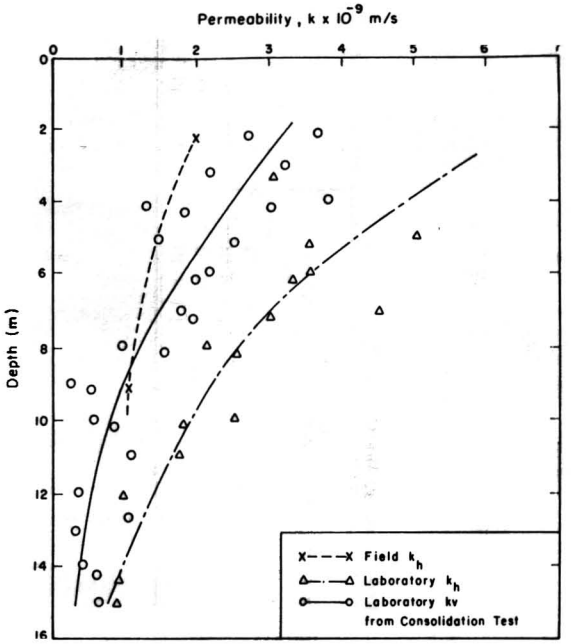

FIG. 6. Variation of Field and Laboratory Permeability with Depth

TABLE 2. Variation of Shear Strength and Deformation Parameters

Depth (m) (1)	E_u (kPa) (2)	c' (kPa) (3)	ϕ' (degrees) (4)
0–2	25,500	8	12.5
2–5	6,600	14	14
5–8	8,933	22	7
8–11	9,120	9	20
11–14	6,593	16	17
14–20	5,884	14	21.5

triaxial tests is discussed in detail by Britto and Gunn (1987). For the current study, the magnitude of λ is selected in such a manner that the undrained experimental stress-strain curve coincides with the undrained predictions from the modified Cam-clay theory.

The values of relevant soil parameters obtained from CK_0U tests and employed in the analysis are summarized in Table 3. The quantity e_{cs} (void ratio at unit P' on an e–ln P' graph) is incorporated instead of N. The variations of bulk modulus (K_w), horizontal and vertical permeabilities (K_h and K_v) with depth are also given. Because intact undisturbed samples from the weathered crust were not recovered for laboratory testing, the Cam-

TABLE 3. Soil Parameters Used in Modified Cam-Clay Model (CRISP)

Depth (m) (1)	κ (2)	λ (3)	e_{cs} (4)	M (5)	ν (6)	K_w ($\times 10^4$) (7)	γ_s (kN/m^3) (8)	k_h (m/s) (9)	k_v (m/s) (10)
0–2.0	0.05	0.13	3.07	1.19	0.3	4.4	16.5	1.5×10^{-9}	0.8×10^{-9}
2.0–8.5	0.05	0.13	3.07	1.19	0.3	1.1	15.5	1.5×10^{-9}	0.8×10^{-9}
8.5–18.5	0.08	0.11	1.61	1.07	0.3	22.7	15.5	1.1×10^{-9}	0.6×10^{-9}
18.5–22.5	0.10	0.10	1.55	1.04	0.3	26.6	16.0	1.1×10^{-9}	0.6×10^{-9}

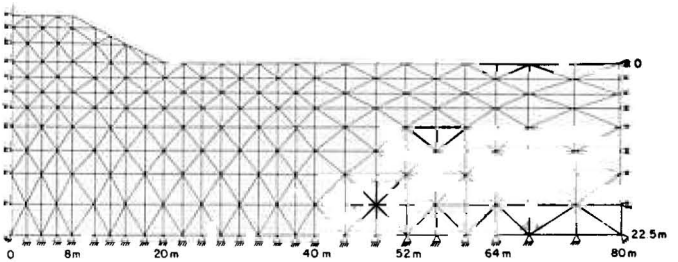

FIG. 7. Finite-Element Discretization of Embankment and Subsoils for CRISP Analysis

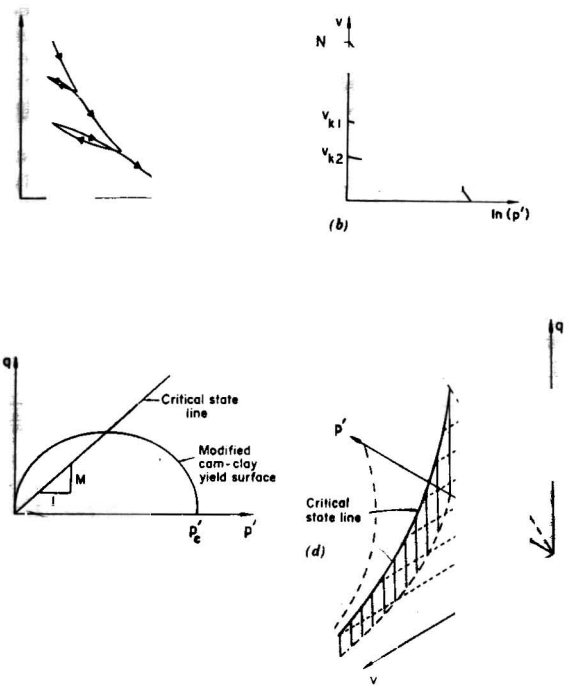

FIG. 8. Critical-State Parameters based on Modified Cam-Clay Model (Britto and Gunn 1987)

clay properties of this topmost layer are assumed to be the same as those obtained for the silty clay layer just beneath it. Since the weathered crust is relatively thin (less than 2.0 m), the errors caused by this assumption are anticipated to be small. In addition to these parameters the in-situ stress conditions are incorporated in the numerical analysis, including the in-situ

effective stresses (K_0), isotropic preconsolidation pressure (P_c'), and the variation of ground-water pressures with depth as summarized in Table 4. The vertical and horizontal permeabilities required for consolidation analysis are interpolated from Fig. 6. For the embankment fill (E = 5,100 kPa; ν = 0.3; and γ = 20.5 kN/m^3), the shear resistance is represented by c = 19 kPa and ϕ' = 26°, obtained from laboratory tests.

Nonlinear (Hyperbolic) Stress-Strain Model in ISBILD

As a supplementary analysis, the nonlinear (hyperbolic) finite-element code, ISBILD (Ozawa and Duncan 1973) is employed. The finite-element-descritization form of the problem applicable for ISBILD is illustrated in Fig. 9, in which isoparametric quadrilateral elements are employed. The stress-strain behavior of a soil depends on a number of different factors including the unit weight, water content, the structure, drainage conditions, loading conditions, duration of loading, and stress history. The soil-deformation response over a wide range of stresses is always nonlinear inelastic, and is dependent on the magnitude of the confining pressure applied in the test. ISBILD was developed on the basis of a hyperbolic (nonlinear) algebraic function, which can be an accurate representation of the soil stress-strain behavior if the necessary parameters can be correctly determined experimentally.

The assumed stress-strain behavior and the required parameters of the hyperbolic model are defined in Fig. 10. For Muar clay a typical failure ratio of 0.86 has been determined from triaxial compression tests. Computation of the tangent modulus, Poisson's ratio, and other properties for

TABLE 4. In-Situ Stress Conditions at Muar Embankment Site

Depth (m) (1)	σ_{ho} (kPa) (2)	σ_{vo} (kPa) (3)	u (kPa) (4)	p_c (kPa) (5)
0	0	0	0	110
2.5	13.2	22.0	16.7	110
8.5	33.7	56.1	75.5	40
18.5	67.9	113.1	173.6	60
22.5	81.5	135.9	212.9	60

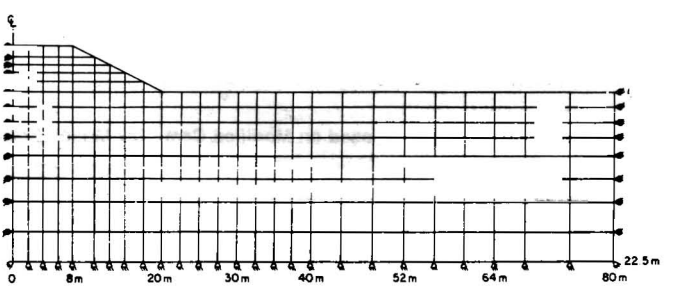

FIG. 9. Finite-Element Discretization of Embankment and Subsoils for ISBILD Analysis

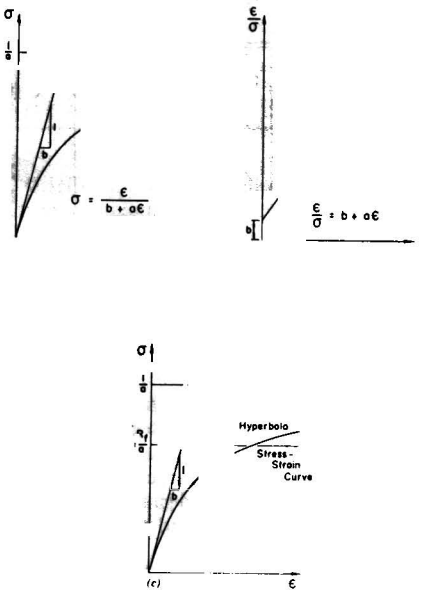

FIG. 10. Parameters Required for Hyperbolic Stress-Strain Model (Ozawa and Duncan 1973)

TABLE 5. Soil Parameters Used for Hyperbolic Stress-Strain Model (ISBILD): Undrained Case

Depth (m) (1)	γ (kN/m³) (2)	K (3)	K_{ur} (4)	c_u (kPa) (5)	ϕ_u (6)
0–2.5	16.5	350	438	15.4	0
2.5–8.5	15.5	280	350	13.4	0
8.5–18.5	15.5	354	443	19.5	0
18.5–22.5	16.0	401	502	25.9	0

the hyperbolic model is explained in detail by Kulhawy et al. (1969) and Ozawa and Duncan (1973). The unloading-reloading modulus number (K_{ur}) is used to evaluate swelling and recompression behavior in addition to the modulus number (K). A summary of soil parameters applicable for undrained and drained analysis by ISBILD is given in Tables 5 and 6.

Finite-Element Analysis

The finite-element method was used to obtain pore-pressure variations beneath the embankment, displacements (vertical and lateral), and surface settlements during each meter of filling, and for subsequent prediction of the failure surface. Shear-stress contours beneath the embankment at failure

TABLE 6. Soil Parameters for Hyperbolic Stress-Strain Model (ISBILD): Fully Drained Case

Depth (m) (1)	γ (kN/m^3) (2)	K (3)	K_{ur} (4)	c' (kPa) (5)	ϕ' (6)
0–2.5	16.5	351	438	8	6.5
2.5–8.5	15.5	390	488	22	13.5
8.5–18.5	15.5	426	533	16	17.0
18.5–22.5	16.0	504	630	14	21.5

are also determined. The predicted results are subsequently compared with the actual field observations. The failure surface was based on the computed yield zones and maximum displacement vectors in the clay subsoils at the critical embankment height of 5.5 m.

Certain simplifications were made in the numerical analysis due to insufficient field or laboratory data for the topmost weathered crust and the relatively deep thin peaty soil layer (Table 1). Some soil properties of the crust are assumed to be the same as those of the upper clay layer deposit due to the absence of intact undisturbed samples for laboratory testing. The effect of the thin peat layer can be ignored because of its considerable depth below the ground level.

The test embankment is compacted with a lateritic fill prone to tensile cracking even at small differential settlements, irrespective of its shear resistance. Tensile resistance of such materials has been discussed in detail elsewhere by Indraratna et al. (1990). The influence of embankment loading is simulated by a constant construction rate of 0.4 m per week to a good approximation, considering a linear elastic analysis with gravity.

Pore Pressure Variations

Within the scope of this paper the responses of five typical piezometers are discussed. They were installed to measure the pore-pressure variations at given locations of the embankment (P2, P3, and P4) and laterally (P2, P5, and P7), as illustrated in Fig. 11. The soft clay beneath the embankment is either normally consolidated or lightly overconsolidated. The prediction of excess pore pressures was performed according to the modified Cam-clay model available in CRISP.

The predicted and observed lateral variations of excess pore pressures (actual and predicted) at locations P2, P5, and P7 with fill thickness are indicated in Figs. 12 (a–c), respectively. It can be observed that the purely undrained analysis overpredicts the pore pressures. As expected, the corresponding predictions from the coupled consolidation analysis are always less than those of the undrained analysis, and are generally in accordance with the measurements. However, at locations P2 and P5 a significant deviation from the measurements is indicated by the coupled consolidation analysis at lower fill heights (less than 2 m), in contrast to the relatively slow rate of pore-pressure development initially observed in the field. This discrepancy may be partly attributed to the fact that at the initial stage the construction of a berm on the west side of the embankment may have temporary reduced the rate of placing of embankment fill. In the analysis, a constant construction rate is assumed. Furthermore, the placement of the fill may subsequently reduce the in-situ permeabilities of the soft clay layer,

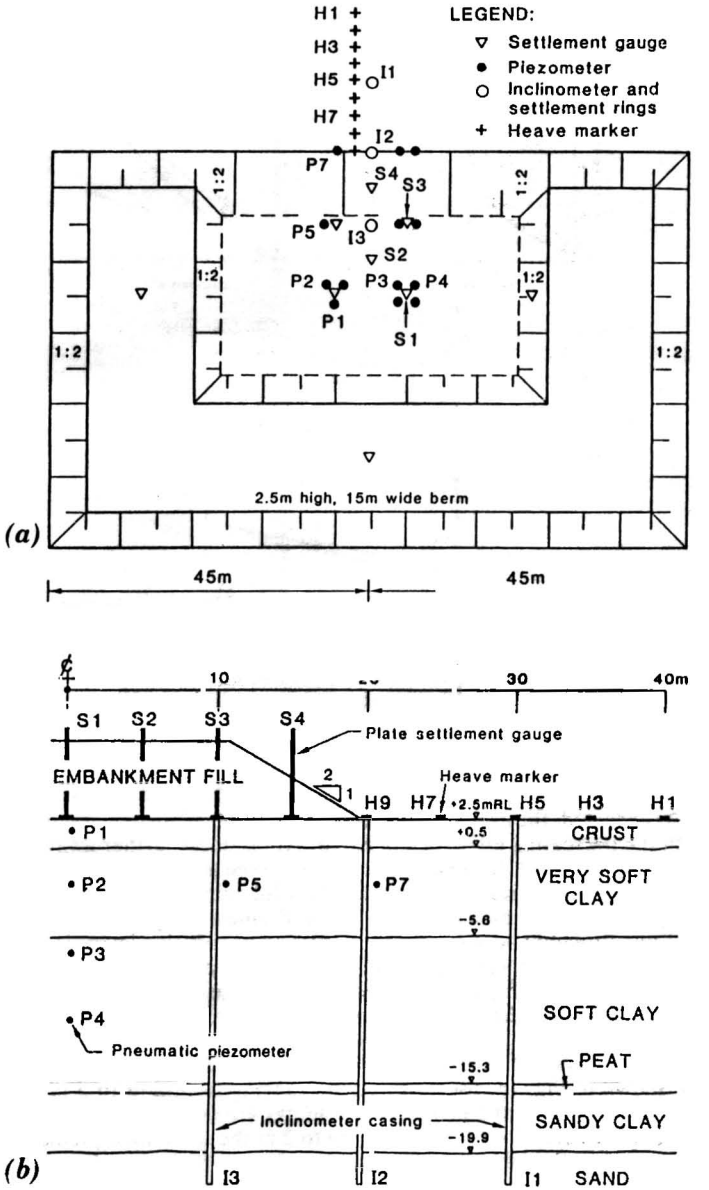

FIG. 11. Plan and Cross Section of Muar Test Embankment Indicating Key Instrumentation

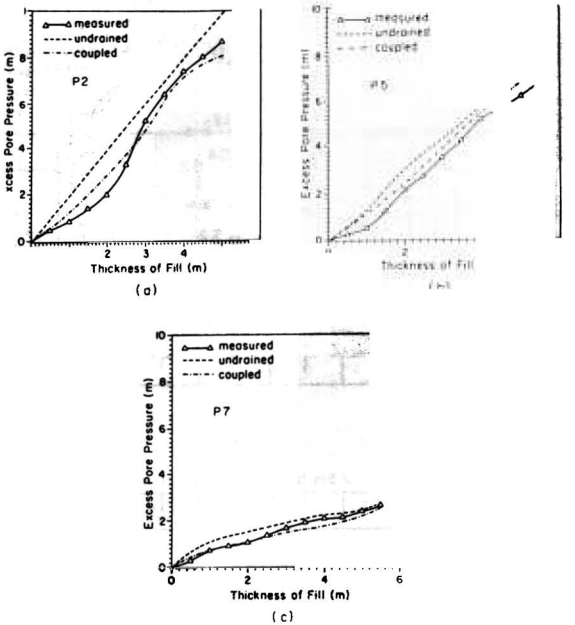

FIG. 12. Lateral Variation of Excess Pore Pressure with Fill Thickness

which in turn would contribute to the higher rate of excess pore-pressure development in the field. In fact, this behavior might be evident at location P2 [Fig. 12(*a*)], as the fill height is raised from 2 m to 4 m.

As expected, the excess pore pressures diminish along the lateral direction with the decreasing effect of surcharge. At distances farther away from the toe (at location P7), the discrepancy between the actual and predicted values (coupled analysis) is insignificant at lower fill heights, in contrast to P2 and P5. Particularly at greater depth, the undrained analysis seems to be less realistic, probably because the consolidation of soft clay layers is promoted by the existence of sandy clay and medium to coarse sand deposits beyond a depth of 18.5 m from the ground level. On the basis of comparison with the observations, the coupled consolidation analysis provides a more acceptable solution.

The variations of excess pore pressures beneath the embankment center are shown in Fig. 13, for fill thickness ranging from 2 m to 5 m. At a fill thickness of 5.5 m, the piezometer readings are not available as a result of complete failure. For fill thickness up to 2 m the undrained predictions are much greater than the measured values, whereas the coupled analysis gives a better estimation. In the vicinity of the ground surface, upward drainage can occur readily, leading to rapid dissipation of the excess pore pressures. Therefore, at locations near the surface, realistic predictions should only be anticipated from the coupled analysis. However, with increased depths, where the dissipation of pore pressures tends to become restrained, the undrained model may also give realistic predictions. For instance, at loca-

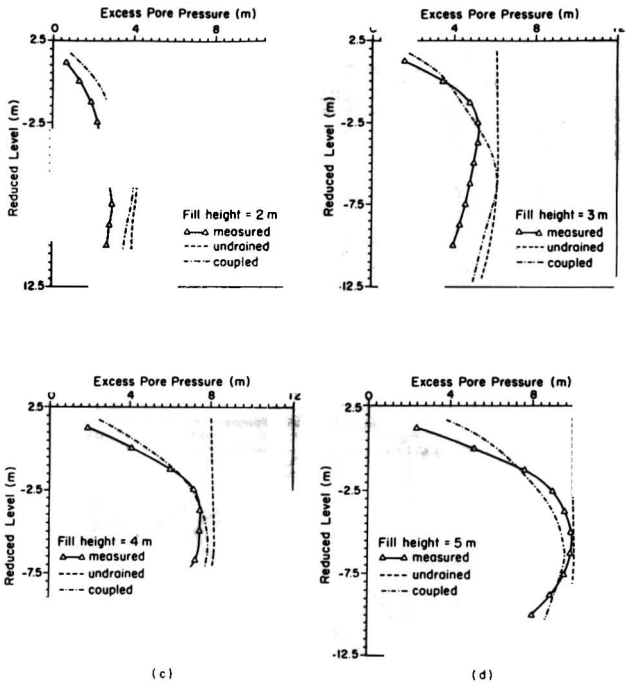

FIG. 13. Variation of Excess Pore Pressures Beneath Embankment Center Line

tions in the vicinity of −7 m RL (reduced level) (i.e. midsection between the ground surface and the bottom sandy layer), the undrained solutions are very close to the measurements. At greater depths, when K_0 conditions are approached and the dissipation of excess pore pressures is promoted by the presence of the sandy clay sandy, a purely undrained analysis is not appropriate. This is particularly true as failure is approached [Fig. 13(*d*)], where the coupled analysis seems to be in good agreement with the measurements.

It must also be realized that the modified Cam-clay model is best represented for normally consolidated and lightly overconsolidated soils with "wet" behavior, where the positive pore pressures cause the water to flow out of the soil. In this study, the deformation behavior of soft Muar clay is always on the "wet side," and thus the modified Cam-clay model is appropriate.

Inception of Failure and Lateral Displacements

The actual slip surface is interpreted by connecting the points of maximum lateral displacements measured by inclinometers I1, I2, and I3, respectively. The inception of failure can be detected best by considering the response of I2 and I3. At these locations the displacement responses are more sensitive during embankment construction in contrast to I1, which is situated 10 m away from the toe. For instance, Fig. 14(*a*) illustrates the variation of

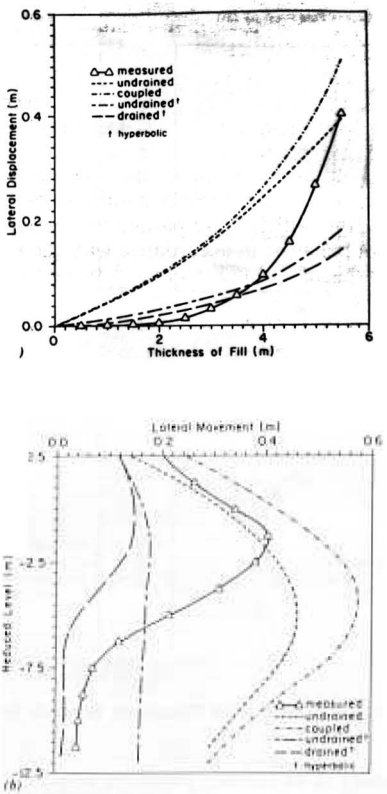

FIG. 14. Variation at Location of Inclinometer, I3: (*a*) Lateral Displacement Response at 4.5 m Depth; (*b*) Lateral Displacement Profile at Failure

lateral displacements for I3 with increasing fill thickness at a depth of 4.5 m, where the displacements increase rapidly as a fill height of 5.0 m is approached. Cracking of embankment fill and ultimate failure were observed in the field at a fill thickness of about 5.5 m. As observed from Fig. 14(*a*), only the coupled consolidation analysis seems to be realistic in predicting the critical height with respect to the variation of displacements, although the computed magnitudes are significantly overestimated, especially at lower fill heights.

The lateral displacement profile with depth for inclinometer I3 at the critical embankment height (5.5 m) is shown in Fig. 14(*b*). As expected, the maximum displacements are measured within the upper, very soft clay layer at a depth of 5 m below ground level. As the deeper (stiffer) deposits are encountered the lateral displacements are severely curtailed. As indicated before, at depths in excess of 12 m below the ground level, a state of K_0 conditions is approached toward the sandy soil deposits. Consequently, while realistic predictions from Cam-clay models can be obtained for the upper, soft clay layer, they deviate from the field behavior at greater depths.

As evident from Fig. 14, the consolidation analysis based on the modified Cam-clay theory generally overestimates lateral displacements. The reason for this discrepancy may be attributed to several factors, including the accuracy of soil parameters, the implications of the associated flow rule (normality condition), and the simulation of plane-strain conditions. In addition, the stiff surficial crusts could have restricted the horizontal deformation beneath the embankment to some extent, which could not be accurately modeled in the analysis. It is found that lateral displacements are also sensitive to nominal changes of λ (Balachandran 1990). In this finite-element analysis (CRISP), the critical-state parameters were obtained from triaxial CK_0U stress-strain behavior in accordance with the modified Cam-clay theory. The magnitudes of soil parameters determined in laboratory are not only influenced by the initial stress conditions but also by the subsequent stress paths followed under given loading-unloading conditions. Although the Cam-clay theory proposes the soil parameters (λ,k, and M) to be unique for a specific yield surface, the laboratory determination of their magnitudes can be influenced by the nature of stress-path testing (Yau 1990).

Surface Settlements and Heave

Typical surface-settlement profiles for incremental fill heights (2–5 m) are shown in Fig. 15. Predictions were made on the basis of both modified Cam-clay and hyperbolic stress-strain models, utilizing the finite-element

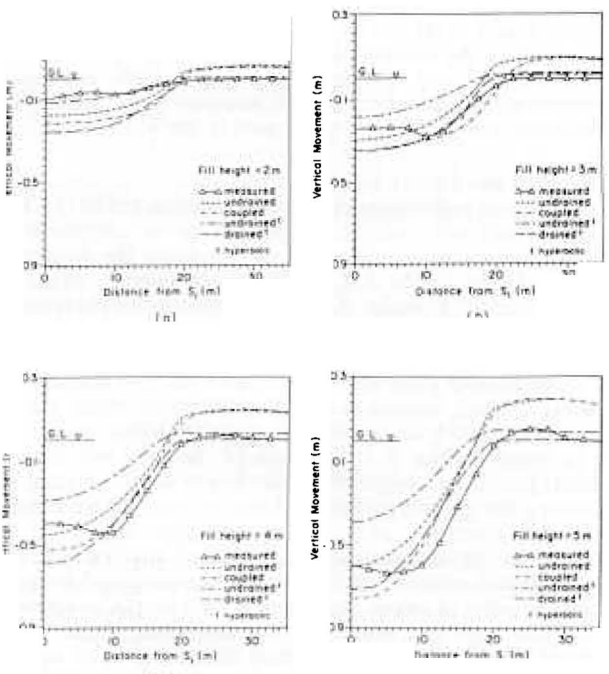

FIG. 15. Surface Settlement Profiles for Various Fill Heights

codes CRISP and ISBILD, respectively. At lower fill heights (up to 2 m), all predictions overestimate vertical settlements; whereas at greater embankment heights, the observed values are in excess of predictions except in the vicinity of the center line of fill. Contrary to expectations, the measurements indicate the occurrence of maximum settlements at a lateral distance of 8–10 m farther away rather than at the center line.

Because the actual field conditions are partly drained, realistic predictions of surface settlement should be anticipated from a coupled consolidation analysis. Nevertheless, for initial embankment heights [e.g. Fig. 15(*a*)], the nonlinear, or hyperbolic, undrained consolidation model gives an acceptable fit to the actual settlement profile for in-situ stresses less than p_{max}. This is not surprising, since at small surcharge loads the total settlements may primarily consist of immediate settlements. Although it is not feasible to generalize as to which constitutive model or consolidation analysis is the most appropriate, it seems that at greater fill heights (3–5 m) the settlement predictions from the coupled consolidation analysis provides realistic solutions. This is expected because at elevated surcharge loads the contribution from consolidation settlements (for stresses exceeding the preconsolidation pressure) becomes significant.

The advantage of using the hyperbolic stress-strain model in predicting heave is obvious. In fact, at fill heights close to failure [Fig. 15(*d*)], the undrained analysis seems to be in better agreement with the measurement. Unfortunately, the modified Cam-clay theory significantly overestimates heave in the vicinity of the toe. As discussed earlier, this discrepancy may be partly attributed to the stress-path sensitivity of soil parameters used in CRISP, as well as the deviations from the assumed flow rule (normality condition) used in theory. To predict heave accurately, loading-extension tests representing the actual stress-path behavior in the vicinity of the toe may yield better soil parameters to be used in the analysis.

Subsoil Yielding and Failure Surfaces

Only the coupled undrained-drained consolidation model of CRISP could predict the overall instrumentation response to an acceptable degree of accuracy. Therefore, within the scope of this paper the evaluation of the critical embankment height and the associated failure surface are based purely on the foregoing model. As the embankment height is increased the extent of subsoil yielding becomes greater. The contour plots of normalized shear stress ratios (shear stress–undrained shear strength) are illustrated in Fig. 16. These contour plots were prepared for fill thickness of 4 m and 5.5 m (at failure), which indicate potential yield zones where the computed shear stresses approach the undrained shear strengths. It is evident that yielding is initiated close to the bottom of the very soft clay layer and subsequently propagates toward the center line as the fill height is increased. By considering the general pattern of these contours, hence identifying the probable failure zones (τ/c_u at 1), the potential shear band propagation can be interpreted in conjunction with the associated displacement vectors.

The inclinometer measurements as well as the predicted lateral displacements from the coupled consolidation model indicate the inception of failure at 5.5 m fill thickness. Due to the high degree of compaction of the lateritic embankment fill, it is not surprising that tensile failure of such materials could take place at extensional strains as small as 0.1–0.25% (Indraratna et al. 1990). Finite-element analysis indicated maximum tensile strains at the base of the embankment ranging from 0.13% to 0.80% as the fill thick-

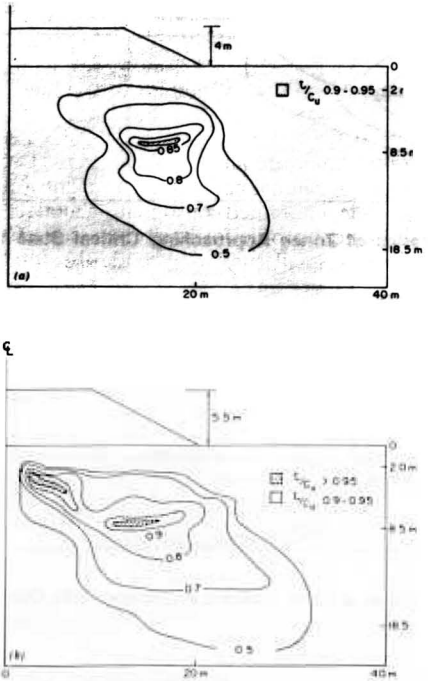

FIG. 16. Contour Plots of Normalized Shear-Stress Ratios

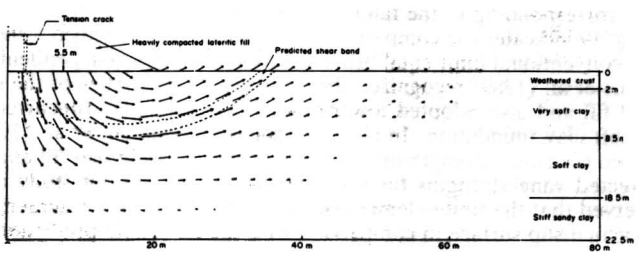

FIG. 17. Maximum Incremental Displacements at Failure

ness was increased from 4.0 m to 5.5 m. The occurrence of a tension mode of failure of the compacted embankment was already mentioned (Fig. 2).

To determine the shear surface through the clay foundation, the maximum incremental displacement vectors were computed along several vertical planes of the finite-element mesh. The predicted shear band interpreted in this manner is shown in Fig. 17. The boundaries of yielded zones approaching

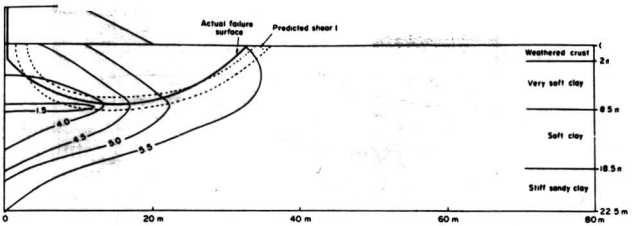

FIG. 18. Boundaries of Zones Approaching Critical State with Increasing Fill Thickness

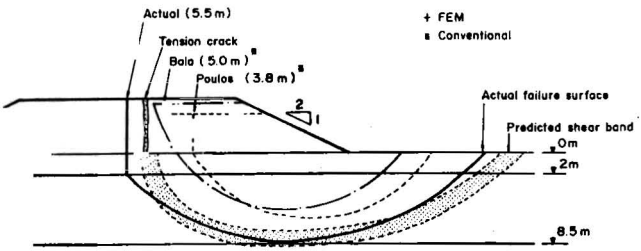

FIG. 19. Comparison of Finite-Element Predictions with Conventional Limit Equilibrium Solutions

the critical state are illustrated in Fig. 18, where each contour indicates the current fill height. In the upper, very soft clay layer the inception of failure is evident by the dramatically extended boundary of the yielded zone at 5.5 m of fill thickness, in comparison with that of 5.0 m. It is verified that the predicted shear band (replotted in Fig. 18) is engulfed within the critical zone corresponding to the failure height of 5.5 m.

Fig. 19 indicates the comparison of the numerically predicted shear band with conventional limit-equilibrium solutions by other independent studies. Poulos et al. (1989) recognized the poor tensile properties of the embankment fill and also adopted lower-bound vane strengths (uncorrected) for the soft clay foundation. In contrast, Balasubramaniam et al. (1989) considered the shear-strength mobilization of the embankment fill and applied corrected vane strengths for the subsoils. In the present study it can be observed that the finite-element solution provides a better agreement with the actual slip surface in comparison with the slip-circle predictions.

Conclusions

The behavior of a soft marine clay foundation subjected to embankment loading can be predicted reliably by the coupled consolidation model. However, the accurate prediction of lateral displacements, and heave in particular, require careful assessment of soil parameters corresponding to the actual stress-path response in the field during embankment loading. For instance, a reliable estimation of parameters with respect to heave at the vicinity of the toe may require loading-extension conditions to be simulated

in triaxial tests, in preference to loading-compression. With regard to the modified Cam-clay model, the associated flow rule in general overestimates postyield displacements. In this respect, application of the continuous plasticity version of the critical-state model (Naylor 1985) or bounding-surface formulation (Dafalias and Hermann 1982) may be promising in describing anisotropic yielding. However, considering the relative simplicity of Cam-clay theories, if one were to employ any complex constitutive model in finite-element analysis, the additional computational efforts should be justified not only by a superior conceptual picture, but also by more realistic numerical predictions.

Purely undrained analysis irrespective of whether it is based on the modified Cam-clay or the hyperbolic stress-strain model is generally not reliable except at central regions of the clay formation, at depths of 7–9 m below ground level. In the vicinity of the ground surface, the dissipation of excess pore pressures is facilitated. At much greater depths toward the sandy soils, not only are the displacements reduced, but also a state of K_0 conditions is approached. Purely undrained deformation analysis is unrealistic for such situations.

The finite-element analysis is capable of predicting the correct mode of failure by considering the incremental displacement vectors and mobilized shear stress contours. The occurrence of excessive tensile strains at the base of the embankment has undoubtedly encouraged cracking of the heavily compacted fill irrespective of its shear strength. In fact, the cracking of the topmost weathered clay crust could also be interpreted in a similar manner if the tensile properties of the crust were available. The predicted shear-band propagation by the finite-element analysis compares well with the observed slip surface. On the other hand, limit-equilibrium methods of analysis are capable of predicting the actual failure surface only if the shear strength of the embankment fill is properly taken into consideration.

It can be envisaged that higher embankments can be raised on soft clay deposits if the tensile mode of failure of the compacted fills can be suppressed. Therefore, the utilization of a backfill with sufficient shear resistance supported by internal reinforcements such as geogrids should be encouraged in the construction of high embankments. Furthermore, the presence of a rigid layer (crust) beneath the embankment can resist lateral displacements, promoting a greater height of fill prior to failure. In effect, this would encourage the use of additives in surface stabilization.

Acknowledgments

The writers gratefully appreciate the assistance provided by Miss E. L. G. Dilema, Mr. N. S. Nilaweera, and Mr. Ranjith Premalal during the preparation of this manuscript. The second writer particularly wishes to thank the Malaysian Highway Authority for inviting him to be one of the four international predictors for the Symposium on Trial Embankments on Malaysian Marine Clays, held in November 1989. The writers also extend their sincere thanks to Mr. Robert Hudson and Dr. E. W. Brand for their technical assistance in numerous ways.

Appendix. References

Balachandran, S. (1990). "Simulation of a test embankment failure (Muar flood plain, Malaysia) using finite element techniques coupled with critical state soil mechanics," thesis presented to the Asian Institute of Technology, at Bangkok,

Thailand, in partial fulfillment of the requirement for the degree of Master of Science.

Balasubramaniam, A. S., Phien-wej, N., Indraratna, B., and Bergado, D. T. (1989). "Predicted behavior of a test embankment on a Malaysian marine clay." *Int. Symp. on Trial Embankments on Malaysian Marine Clays,* Kuala Lumpur, Malaysia, Vol. 2, 1-1–1-8.

Bjerrum, L. (1973). "Problems of soil mechanics and construction on soft clays. State-of-the-art report to Session IV." *8th Int. Conf. on Soil Mech. and Found. Engrg.,* Moscow, U.S.S.R.

Brand, E. W., and Premchitt, J. (1989). "Moderator's report for the predicted performance of the Muar test embankment." *Proc., Int. Symp. on Trial Embankment on Malaysian Marine Clays,* Kuala Lumpur, Malaysia, Vol. 2, 1/32–1/49.

Britto, A. M., and Gunn, M. J. (1984). *CRISP user's and programmer's guide.* Cambridge University, Cambridge, England.

Britto, A. M., and Gunn, M. J. (1987). *Critical state soil mechanics via finite elements.* Ellis Horwood, Chichester, England.

Dafalias, Y. F., and Herrman, L. R. (1982). "Bounding surface formulation of soil plasticity." *Soil mechanics—transient and cyclic loads* G. N. Pande and O. C. Zienkiewicz, eds., John Wiley and Sons, New York, N.Y., 253–282.

Indraratna, B., Dilema, E. L. G., and Nutalaya, P. (1990). Suitability of lateritic residual soil for core compaction and design of appropriate granular filters. *Dam Engrg.*, 1(3), 201–220.

Kulhawy, F. H., Duncan, J. M., and Seed, H. B. (1969). "Finite element analysis of stresses and movements in embankments during construction." *Contract Report No. S-69-8, USAEWES*, Vicksburgh, Miss.

Naylor, D. J. (1975). "A continuous plasticity version of the critical state model." *Int. J. Num. Meth. in Engrg.*, 21(7), 1187–1204.

Ozawa, Y., and Duncan, J. M. (1973). *ISBILD: A computer program for static analysis of static stresses and movement in embankment.* University of California, Berkeley, Calif.

Poulos, H. G., Lee, C. Y., and Small, J. C. (1989). "Prediction of embankment performance on Malaysian marine clays." *Int. Symp. on Trial Embankments on Malaysian Marine Clays*, Kuala Lumpur, Malaysia, Vol. 2, 1-22–1-31.

Proc., Int. Symp. on Trial Embankments on Malaysian Marine Clays, (1989). Malaysian Highway Authority, Kuala Lumpur, Malaysia.

Roscoe, K. H., and Burland, J. B. (1968). "On the generalized stress strain behavior of wet clay." *Engineering plasticity.* Cambridge University Press, Cambridge, England.

Roscoe, R. H., and Poorooshasb, H. B. (1963). "A theoretical and experimental study of strains in triaxial tests on normally consolidated clays." *Geotechnique*, London, England, Vol. 13, 12–38.

Yau, K. F. (1990). "Stress paths below embankments and excavations in Bangkok subsoils, thesis presented to the Asian Institute of Technology, at Bangkok, Thailand, in partial fulfillment of the requirements for the degree of Master of Science.